

study area in the southwest accompanied by an increasingly steep gradient. The precipitous dropoff of nearly 61 m (200 ft) of water table elevation in the southwest causes streamlines to converge in this area.

The inclusion of NWIS data to supplement the INL-collected data provides real points to control the shape of computer-generated contour lines at the distal portions of the study area. This has led to re-thinking the model domain. Using the high-density INL-collected water levels around the facilities provides greater control of streamline direction, with results more consistent with concepts of groundwater flow arising from the interpretation of sampled contaminant concentrations in the aquifer.

June 2005 OU 10-08 Water Level Measurements—Water levels in nearly 300 wells were measured over a three-day period in June 2005 (see Figure 2-24). This represents an improvement in the sitewide collection process over June 2004. However, the June 2005 water table contour map is still under development. During the fiscal year 2005 effort, the June 2004 map was studied extensively, and minor changes were made to reflect better data and a better understanding of the groundwater flow field at or near the INL Site. A water table map not only provides a picture of groundwater movement but also provides input in the selection of the model domain, boundary types, and boundary locations.

2.3.2 Geochemistry

Geochemical data are being used to evaluate the rate and direction of groundwater flow to eventually constrain the groundwater transport model results and for comparison to simulated flow paths for the two-dimensional model described in Section 3. These geochemical data include water chemistry analyses for anthropogenic and naturally occurring constituents that serve as chemical tracers in groundwater.

2.3.2.1 Anthropogenic Tracers. Federal and state agencies, universities, and private contractors have monitored the INL Site extensively since 1949 to evaluate the distribution and transport of contaminants in groundwater. In 2003, contaminated groundwater at the INL Site has been detected at the RWMC, RTC, INTEC, TAN, and Central Facilities Area (CFA) (Figure 2-29). At TAN, trichloroethene was the primary constituent exceeding its maximum contaminant level (MCL), but cis-1,2-dichloroethene (-DCE), trans-1,2-DCE, and tetrachloroethene also exceeded their respective MCLs. Sr-90, Tc-99, and gross alpha exceeded their respective MCLs at and near INTEC. Chromium exceeded its MCL in water in two wells south of the RTC. Nitrate exceeded its MCL in two wells south of CFA. Carbon tetrachloride exceeded its MCL in groundwater beneath the RWMC.

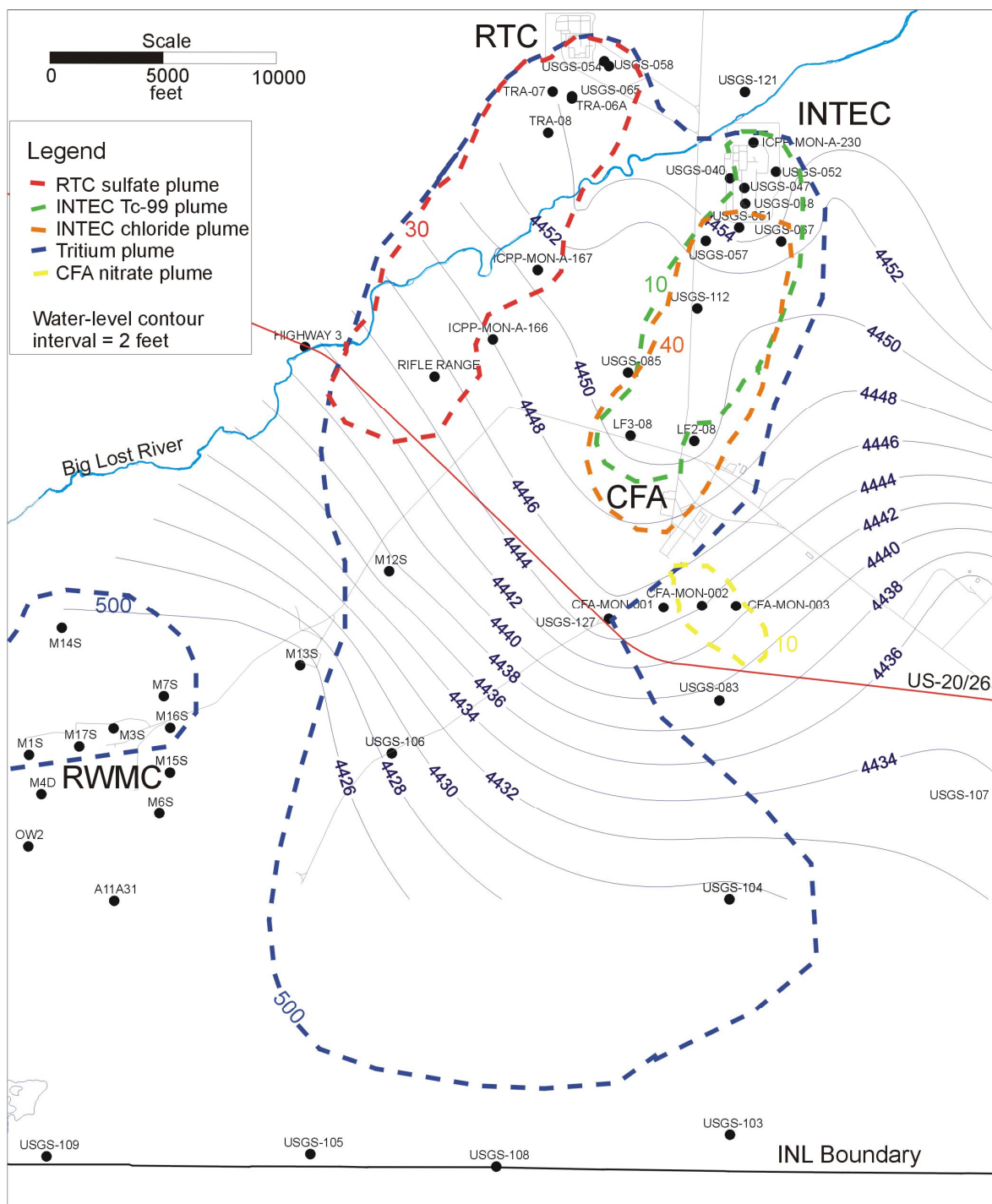
In addition to contaminants above the MCL, several other anthropogenic contaminants form the following plumes:

- At INTEC: tritium, I-129, Tc-99, Sr-90, chloride, nitrate, and sodium
- At CFA: nitrate, chloride, tritium, and sodium
- At RTC: chromium, tritium, and sulfate
- At RWMC: carbon tetrachloride, tritium, anions (chloride and sulfate), and trichloroethene
- At TAN: trichloroethene, tetrachloroethene, DCE, Sr-90, and tritium.

Selected plumes in the RTC/INTEC/CFA/RWMC area are shown on Figure 2-30 to illustrate groundwater flow paths, the potential for commingling plumes, and the possibility of upgradient influence on the RWMC. The contaminant distributions in the SRPA generally agree with groundwater flow paths indicated by the water-level contours. However, the upgradient influences on the RWMC from the RTC and INTEC are uncertain. If there is a contribution, it is within the scope of OU 10-08 to account for the effects of commingling plumes as defined in the OU 10-08 RI/FS.



Figure 2-29. Contaminant plumes with concentrations exceeding maximum contaminant levels in 2003.



and Cl-36 studies were analyzed using the low-detection limit accelerator mass spectrometry method; samples collected for Tc-99 studies were analyzed using the thermal ionization mass spectrometry method. The results are described below. I-129 and Cl-36 are excellent tracers for groundwater flow and contaminant migration paths. Cl-36 is an excellent tracer, because it is a conservative anion, and I-129 is an excellent tracer in anion form. In addition, I-129 and Cl-36 can be tracked over great distances.

A Cl-36 plume extending from the RTC and INTEC to the southern INL Site boundary is described in two studies (Beasley et al. 1993; Cecil et al. 2000). A comparison of tritium and Cl-36 data indicated that the Cl-36 plume extended beyond the area of the tritium plume defined by the 500-pCi/L concentration for tritium. Cl-36 was also detected in a well at the RWMC (Beasley et al. 1993). Based on the first detection of Cl-36, contaminant/groundwater flow velocities of approximately 1 m/day (3 ft/day) were estimated for two wells south of the INL Site boundary (Cecil et al. 2000).

Sampling done in 1991 and 1992 identified an I-129 plume extending from INTEC to south of the INL Site boundary (Mann and Beasley 1994). It should be noted that the I-129 concentrations south of the INL Site boundary are low (at least two orders of magnitude below the MCL of 1 pCi/L). Groundwater flow velocity from INTEC past the southern boundary of the INL Site was estimated at 1.8 m/day (6 ft/day) based on movement of I-129 (Mann and Beasley 1994). I-129 was also detected at low concentrations in USGS-90, which is located near the RWMC (Mann and Beasley 1994). The occurrence of a low I-129 concentration near the RWMC suggests that a groundwater flow path from INTEC exists and that INTEC/RWMC plumes could be commingling. The interpretation of flow paths is complicated, because I-129 is also present in the wastes emplaced in the RWMC. Sampling of Magic Valley wells and springs south of the INL Site from 1992 to 1994 indicated background I-129 concentrations (Cecil et al. 2003). Although a Cl-36 plume originates from both the RTC and INTEC, I-129 appears to originate from INTEC but not from the RTC (Mann and Beasley 1994). In addition to samples collected during the Mann and Beasley study, I-129 samples were collected south of INTEC in 1977, 1981, 1986, and 1990.

Sampling and analysis for Tc-99 using the low-detection limit thermal ionization mass spectrometry method indicated a plume from INTEC extending past the southern boundary of the INL Site (Beasley et al. 1998). Tc-99 was detected in the RWMC production well, which is consistent with the low-detection limit I-129 data. This suggests that a groundwater flow path extends from INTEC to the RWMC and that commingling of INTEC and RWMC contaminant plumes is possible. The interpretation of flow paths is complicated, because Tc-99 is also present in the wastes emplaced in the RWMC.

In addition to the radiological analytes discussed above, the USGS has mapped concentrations of chlorofluorocarbons (CFCs) in the SRPA (Busenberg et al. 2001). The CFC analyses were done to estimate the age of groundwater beneath the INL Site, but they indicated the presence of several CFC anomalies that could potentially be used as groundwater flow tracers. The CFC study indicated a plume of dichlorodifluoromethane (F-12) originating from INTEC and a 1,1,2-trichloro-1,2,2-trifluoroethane (F-113) plume originating at the RWMC. However, the CFC concentrations were very low and required special detection methods (Busenberg et al. 2001).

OU 10-08 Geochemical Study—A geochemical study in progress will attempt to resolve the source of the tritium in the aquifer at the RWMC, identify flow paths of contaminants from INTEC and the RTC, determine the source of the anion anomaly south of the RWMC, and identify flow paths and evaluate contaminant influence south of the southern INL Site boundary (Figure 2-31). Identification of groundwater flow paths is essential for development and calibration of the SWGM. In addition, data from the geochemical study will be used to evaluate the potential for commingled plumes, which might elevate the cumulative risk above levels calculated for each plume individually.

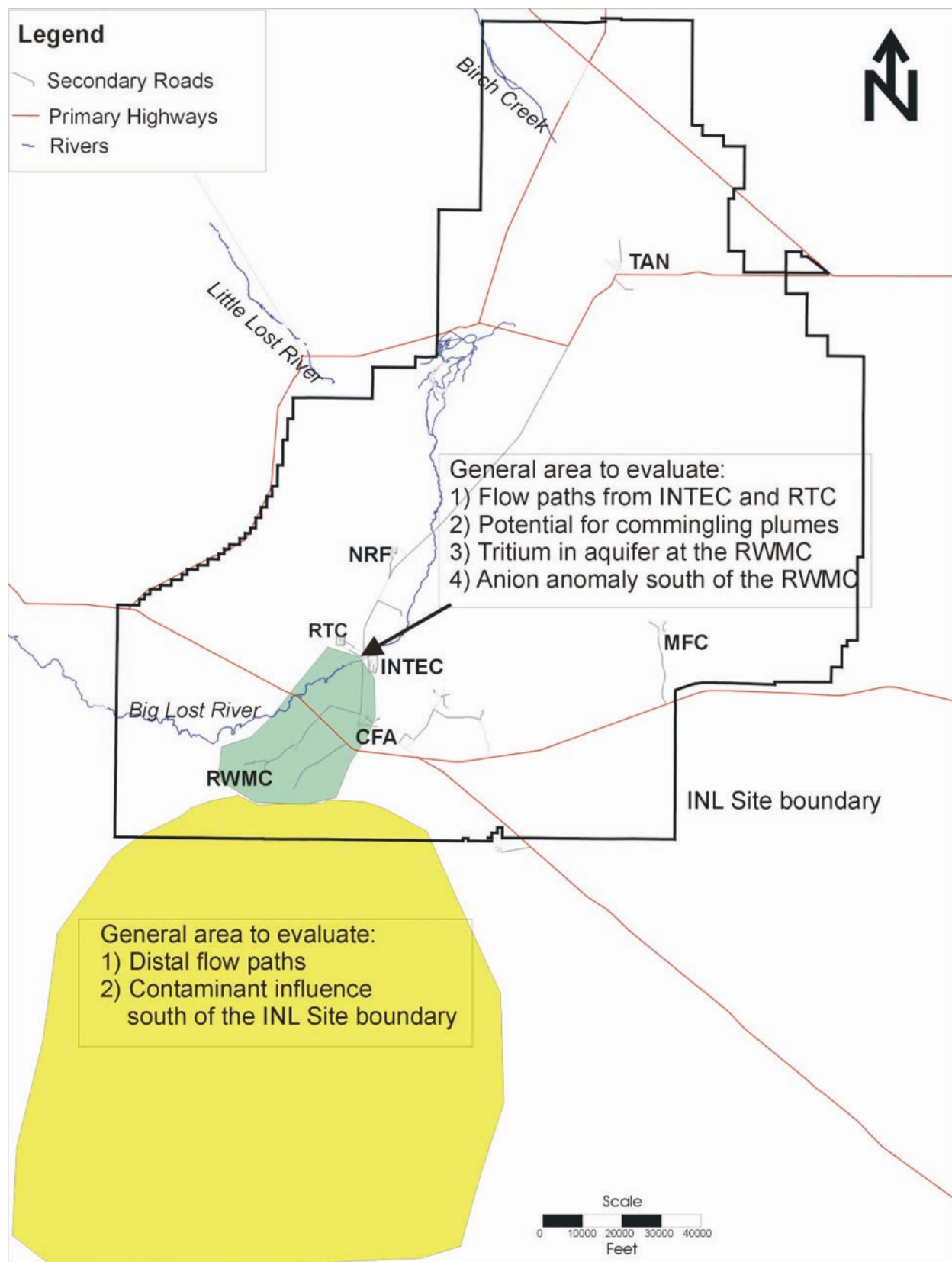


Figure 2-31. Geochemical study areas.

2.3.2.2 Preferential Flow. Since the earliest studies of the SRPA, researchers have recognized that aquifer temperature and the chemical signature of groundwater are useful tools in characterizing the aquifer flow system (Olmsted 1965). As the number of studies and available data have increased, more insight into the nature of the aquifer system has been gained. Specifically, beginning in 1997, a series of investigations has been conducted to characterize groundwater flow in the context of the regional geologic framework that hosts the aquifer. These studies investigated aquifer temperature distribution, natural groundwater isotopes, and chemistry as indicators of preferential flow paths. Aquifer isotope signature, major element geochemistry, and temperature distribution have revealed the presence of zones in the aquifer that have been interpreted as preferential flow corridors that are surrounded by zones of slower flow. Because of the INL Site's proximity to the northwestern boundary of the ESRP, a number of sources and types of water contribute recharge to the system. These sources include infiltrated irrigation water, the Big Lost River Valley, the Little Lost River Valley, the Birch Creek Valley, the Mud Lake basin, and, the largest contributor, the Yellowstone Plateau. Another source of water is upwelling of thermal water emanating from deep within the ESRP (McLing et al. 2002; Mann 1986). Because of the distinct chemical and thermal signature of these recharge waters, they can be used as natural tracers to elucidate regional groundwater flow and, therefore, as calibration targets for flow and transport models.

Isotope Delineated Flow Paths—Isotope and chemical tracer studies have addressed the primary concern that, within the aquifer, long-range (tens to hundreds of kilometers) “fast paths” exist that could transport contamination downgradient faster than expected. Isotopes of heavy elements such as those in the uranium and thorium series are powerful tools that can be used to elucidate physico-chemical, geologic, and hydrologic variables of groundwater systems. Because of their high atomic mass, these elements do not fractionate in aquifer systems. These isotopes are very useful, because, in rocks older than a few hundred ka, the ratios of U-234/U-238 are generally close to the secular equilibrium value of 5.49×10^{-6} . In recently recharged groundwater, however, U-234 is typically enriched relative to U-238 by factors most commonly ranging from 1.5 to 10 because of preferential dissolution of U-234 from crystallographic defects created by alpha recoil and because of direct ejection of U-234 into groundwater by recoil (Osmand and Cowart 1992). Variations in U-234/U-238 in short-residence waters (ten to a few hundred years), such as those in the SRPA, reflect the competing effects of aquifer residence time and host rock dissolution. The longer a recharged water with an elevated U-234/U-238 ratio is in contact with the aquifer host rock, the closer to equilibrium it will be.

Strontium isotope (Sr-87/Sr-86) ratios in groundwater reflect the water-rock reaction histories and flow pathways of the water. Groundwater Sr-87/Sr-86 ratios are inherited from soil or rock through which the water passes. Both Sr-87 and Sr-86 are stable isotopes, but because Sr-87 is produced by radioactive decay of Rb-87 ($t_{1/2} = 4.8 \times 10^{10}$ yr), the Sr-87/Sr-86 ratios of rocks and soil depend on their original rubidium concentrations and their ages. For this reason, strontium isotopes are useful as groundwater tracers in a system like the ESRP, because the rock types in the recharge regions are different than the aquifer host rock. Like U-234/U-238, the strontium isotope ratio inherited from the recharge region will evolve toward isotopic equilibrium with the aquifer host rock. The rate at which this equilibration will occur is largely a function of the amount of time that the groundwater is in contact with the aquifer host rock.

Contour plots of uranium and strontium isotope ratios (Figure 2-32) show that water entering the aquifer from the river valleys to the northwest has high ratios of Sr-87/Sr-86 (> 0.71100) and U-234/U-238 and elevated concentrations of thorium. In some areas, the high isotope ratios of this water persist 19 to 30.5 km (12 to 19 mi) downgradient in the aquifer along zones of preferential flow. In contrast, two zones have relatively low Sr-87/Sr-86, U-234/U-238, and Th-234/Th-238 ratios in the central part of the INL Site, one near the southern extent of the Lemhi Range and one near the western boundary of the site near the southern end of the Lost River Range (Figure 2-32).

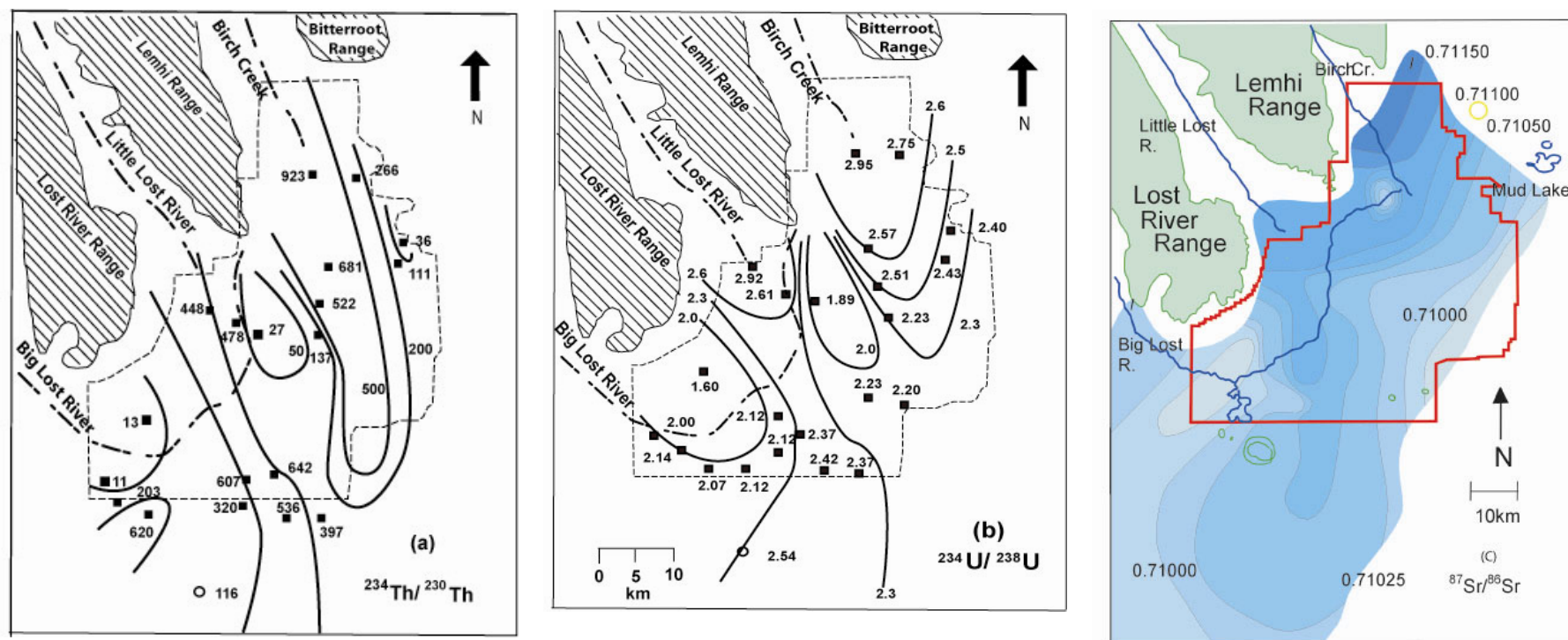


Figure 2-32. Distributions of (a) $^{234}\text{Th}/^{230}\text{Th}$, (b) $^{234}\text{U}/^{238}\text{U}$, and (c) $^{87}\text{Sr}/^{86}\text{Sr}$ activity ratios in INL Site groundwater, all showing southward decreases along two preferential flow paths with minimum values occurring just south of the Lost River and Lemhi ranges. The general similarities among the three plots reflect a linkage between the age of water and areas of preferential flow and stagnant flow. The plot shows that the observed isotopic compositions cannot be explained by mixing of the water masses (after Luo et al. 2000).

Preferential flow of groundwater through the high-ratio zones and relatively long residence time or slow flow through the low-ratio zones can account for the observed isotope-ratio pattern. In this scenario, the high-ratio zones are fast-flow zones, where high-ratio isotopes originating in the recharge zones north of the INL Site persist far into the regional aquifer system, because the groundwater in these preferential flow corridors is moving fast and has had less time to react with the aquifer host rock. In contrast, groundwater in the low-isotope ratio zones evolves closer to the isotopic composition of the host rock— $\text{Sr-87/Sr-86} = 0.7070 \pm 0.0003$ (Leeman and Manton 1971; Morse and McCurry 1997) and $\text{U-234/U-238} \sim 5.49 \times 10^{-5}$ (Roback et al. 2001)—due to slower groundwater flow, longer residence times, and subsequent dissolution of the basalt host rock. Geochemical modeling and temperature profiles supporting this conclusion suggest that groundwater located at the toes of the Lost River and Lemhi ranges is moving slower relative to flow through the rest of the aquifer (Luo et al. 2000), with calculated residence times for water in these “stagnant” zones being two to 10 times longer than in the high-isotope ratio zones (Figure 2-32).

Hydraulic Head versus Chemically Defined Flow Paths—Since the SRPA was first characterized in the mid-1900s, little has changed with respect to the generally accepted northeast-to-southwest flow direction in the SRPA. However, as more wells have been drilled and more studies have been conducted, especially at the INL Site, it has become apparent that the regional potentiometric surface may not have enough resolution in areas with sparsely populated wells to reveal the preferential flow pathways identified by recent geochemical studies. These preferential flow paths indicate that there is a strong geologically based hydraulic anisotropy in the aquifer. Isotope-delineated flow pathways are generally oriented in a northwest-to-southeast direction, which is consistent with the orientation of primary volcanic features on the ESRP (Rodgers et al. 1990). In addition, it is consistent with the Welhan and Reed (1997) predictions of preferred northwest-to-southeast hydraulic conductivity. However, because of the assumptions made in the definition of the preferential flow corridors (i.e., water samples are representative of the entire thickness of the aquifer, and well density is sufficient to define flow corridors), it is not possible to make definitive statements about the cause or exact boundaries of the preferential flow corridors.

Groundwater temperatures and borehole temperature profiles provide another useful tool for ascertaining the geometry of the SRPA and generally support the conclusions of the isotope-preferred flow path studies (Roback et al. 2001; Johnson et al. 2000; Luo et al. 2000). For example, groundwater temperature at the top of the SRPA beneath the INL Site ranges from less than 8°C to more than 18°C (Figure 2-33). The coldest of this water correlates with the preferential flow corridors identified by Roback et al. (2001) and is associated with areas where cold recharge moves rapidly through the system. In contrast, regions with warmer water temperatures generally correlate with the slower flow regions identified by the previous studies (Luo et al. 2000; Roback et al. 2001). This supports the conclusion that areas where water temperature is higher groundwater flow is slow enough that the thermal gradient of the ESRP overwhelms flow velocity.

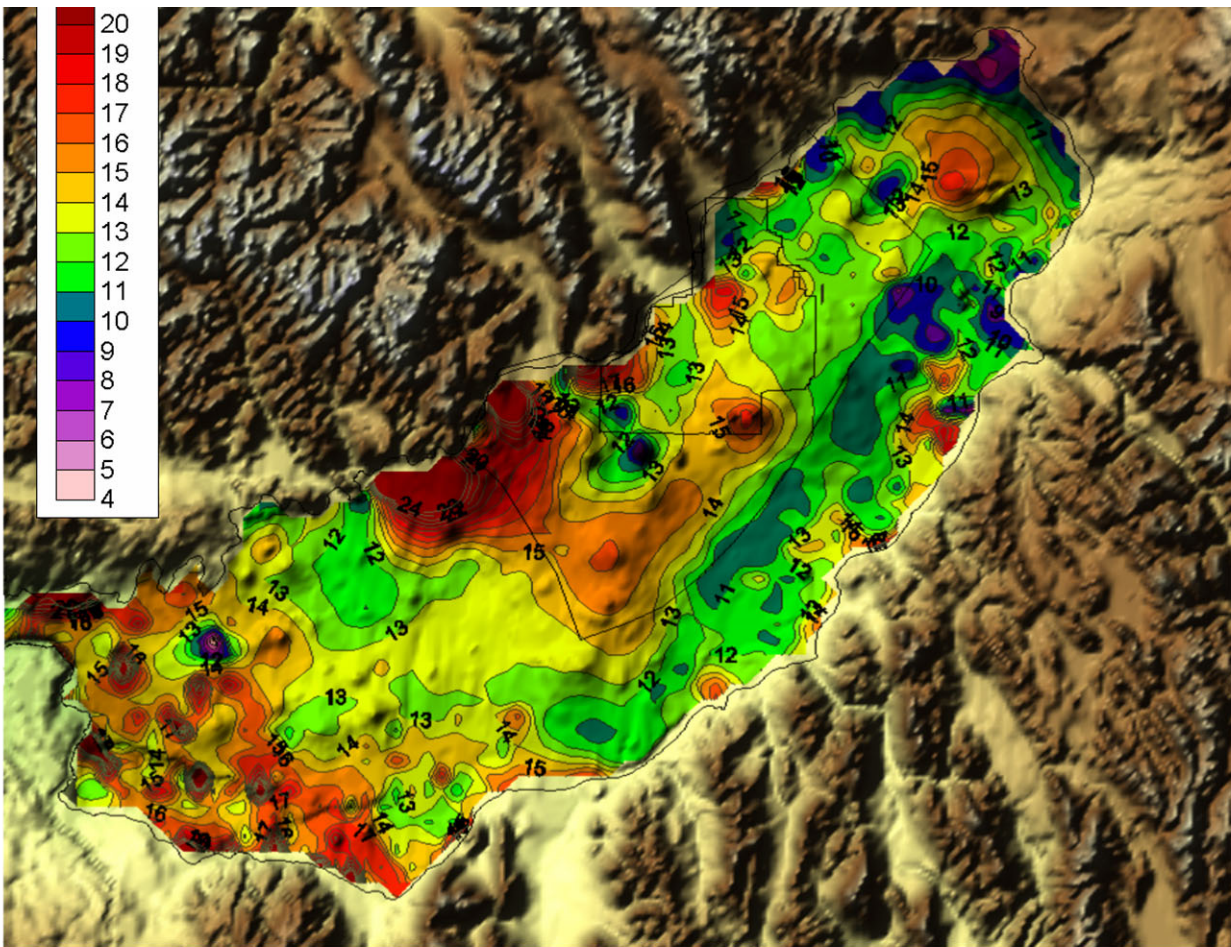


Figure 2-33. Groundwater temperature (°C) in the eastern SRPA, based on groundwater temperature data obtained from the NWISWeb Data for Idaho (<http://nwis.waterdata.usgs.gov/id/nwis/nwis>).

Although the use of natural flow indicators (e.g., chemistry, isotopes, and temperature) are powerful tools for the interrogation of aquifer flow properties, one limitation of this type of data is the lack of spatially distributed data. At the INL Site, most of the wells available for sampling are located near major facilities and are completed in the uppermost part of the SRPA. The same types of problems are encountered using anthropogenic contaminants as tracers. This property of the aquifer-monitoring system at the INL Site creates a data set with a high density of wells in some areas and a paucity of wells in others. As a result, flow fields or pathways based on non-anthropogenic and anthropogenic flow indicators often require significant smoothing or extrapolation on the distal or edge portions of the data set. In some places, this generates significant discrepancies between anthropogenic plume geometries and naturally occurring isopleths. Potential solutions for this problem include more spatially located sampling wells and wells that sample more than just the top of the aquifer. Additionally, it would be beneficial to integrate the natural and anthropogenic data sets such that each set of conclusions is considered in the context of both (a) short-term migration (< 60 years using contaminant plumes) and (b) long-term migration (> 60 years using naturally occurring chemical tracers).

The spatial distribution of water temperature at the top of the SRPA indicates that locally recharged water is not vertically mixed within aquifer but is spread laterally over the upper part of the aquifer (for example, cool water beneath the INL Site spreading areas and the Big Lost River). The effect of locally layered water on the three-dimensional geochemistry of the active SRPA is not well defined.

There is some indication that current well completions at the INL Site result in water samples that are representative of only the most conductive horizon in the completed interval. This has resulted in the assumption that the SRPA is homogeneous vertically and chemically. The need for wells that can be sampled at multiple intervals to provide insight into the vertical chemical stratigraphy of the aquifer is significant.

2.3.3 Temperature

One of the goals of the OU 10-08 modeling program is to use nontraditional data sets to help constrain hydraulic properties in the aquifer. Temperature data, for example, can be used to trace groundwater movement, because the mechanisms of energy transport are essentially the same as those that transport solutes. So if water with a temperature different than the background temperature of an aquifer is introduced at a known location, then the attenuation of that thermal energy difference with time or distance can be modeled just as attenuation of a solute injection can be modeled. Temperature data for the SRPA are thus being collected to attempt to identify the heat sources and sinks and the downstream temperature distributions that may be used to quantitatively estimate groundwater flow velocities using a numerical heat transport simulator.

To map temperature distribution in the SRPA in the vicinity of the INL Site, we rely primarily on two types of data: (1) groundwater temperature measurements that have been collected during water-quality sampling or other monitoring programs and generally represent an integrated temperature for the well and (2) temperature profiles collected during geophysical well logging. The first type, which is far more abundant, is used to define the general two-dimensional (in the horizontal plane) temperature distribution. The second type is used in conjunction with the two-dimensional data to attempt to define the three-dimensional temperature distribution of the system.

2.3.3.1 Spatial Distribution—Horizontal Plane. Groundwater temperature measurements are relatively abundant in the SRPA. The USGS NWISWeb (<http://nwis.waterdata.usgs.gov/id/nwis/nwis>) contains temperature measurements for approximately 5,700 locations in the eastern SRPA. Those data typically contain multiple measurements, at different times, for each well or surface water location. To date, we have used the average of each time series to construct a map of groundwater temperature for the aquifer (Figure 2-33), based on the fact that temperatures respond relatively slowly to changes at the boundaries of the system. Subsequent efforts will focus on examining the variability of temperatures in the SRPA as a means of identifying potential errors and identifying temperature variations characteristic of a seasonal groundwater recharge signal.

The groundwater temperature map produced from the NWIS data illustrates several characteristics that have been noted in several previous studies (Blackwell et al. 1992; Brott et al. 1981). First, temperatures generally increase in the direction of groundwater flow. Recharge temperatures along the edge of the Yellowstone Plateau are approximately 5 to 9°C, while temperatures at the other end of the system, in the vicinity of Thousand Springs, are approximately 15°C. The increase is, however, not a gradual trend with distance. Temperatures increase dramatically over relatively short distances in the northeast part of the system, with a localized warm anomaly located approximately at Grassy Ridge near the Saint Anthony sand dunes. Horizontal temperature gradients around that high temperature anomaly are much greater in the southwesterly direction, perhaps due to agricultural introduction of cold water recharge to the southwest. Groundwater temperatures southwest of that location appear to reflect mixing of water heated by local geothermal effects with water recharged through irrigation or losing streams.

Groundwater temperatures along the northern boundary of the INL Site are approximately 12 to 13°C, and that range is also prevalent throughout parts of the site, to the southeast of the site, and to the southwest of the WAG 10 study area southeast of the Wood River Valley. On, and to the southwest of,

the INL Site, temperatures are locally both higher and lower than that apparent background range. Warm anomalies at several locations appear to reflect local heating, presumably due to areas with greater upward flux of geothermally heated groundwater. Localized hot spots are evident below Craters of the Moon National Monument, along the AVH southwest of the INL Site, and around CH-1 near Middle Butte, where shallow groundwater temperatures reach ~19°C. Two localized cold water anomalies exist in two places in the southwest portion of the INL Site, one located approximately under the Big Lost River spreading areas and a second located directly below Big Southern Butte.

2.3.3.2 Vertical Heat Flux. Vertical heat fluxes above the SRPA provide evidence of the effect of groundwater flow on geothermal heat flow and provide a useful boundary condition for heat flow modeling of the system. To calculate the vertical heat flux distribution over the ESRP, we apply Fourier's steady-state law of heat conduction, as follows:

$$J = -\kappa_{eff} \frac{\Delta T}{\Delta Z} \quad (2-1)$$

where

- J = heat flux
- κ_{eff} = effective thermal conductivity
- ΔT = temperature difference (mean annual air temperature minus groundwater temperature)
- ΔZ = elevation difference (ground-surface elevation minus water table elevation).

The heat flux calculation, therefore, requires spatial distributions of groundwater temperature, surface temperature, water table elevation, and ground surface elevation. For this system, we assumed a ground surface temperature equal to the mean annual air temperature for the area (using gridded data obtained from the Spatial Climate Analysis Service [2005], Oregon State University), estimated groundwater elevations from the 1980 water table map developed by Garabedian (1992), and ground surface elevations from a USGS digital elevation model for the region. We assumed an effective thermal conductivity of 2 watts m⁻¹ K⁻¹, a reasonable approximation for basalt (e.g., Brott et al. 1981).

Resultant heat fluxes are generally upward across the ESRP, even in the recharge areas at the edge of the Yellowstone Plateau (Figure 2-34). The persistence of upward heat fluxes throughout the northeastern portion of the ESRP contradicts the conclusions of some previous studies (Brott et al. 1981; Blackwell et al. 1992) that described heat fluxes as positive in that vicinity. This suggests that mountain-front recharge is generally warmer than the mean annual air temperature. With one exception, calculated heat fluxes were negative only where the water table elevation exceeded the ground surface elevation, indicating errors in the elevation data used. The high positive heat fluxes surrounding those areas may thus, to some extent, reflect errors in the groundwater elevation data if the thickness of the vadose zone is substantially underestimated. In this case, the groundwater elevation data are based on a water table map developed by Garabedian (1992) for 1980 water levels. The sensitivity of the calculated heat flux to elevation differences suggests that further effort should be made to develop a more accurate water table map for the aquifer.

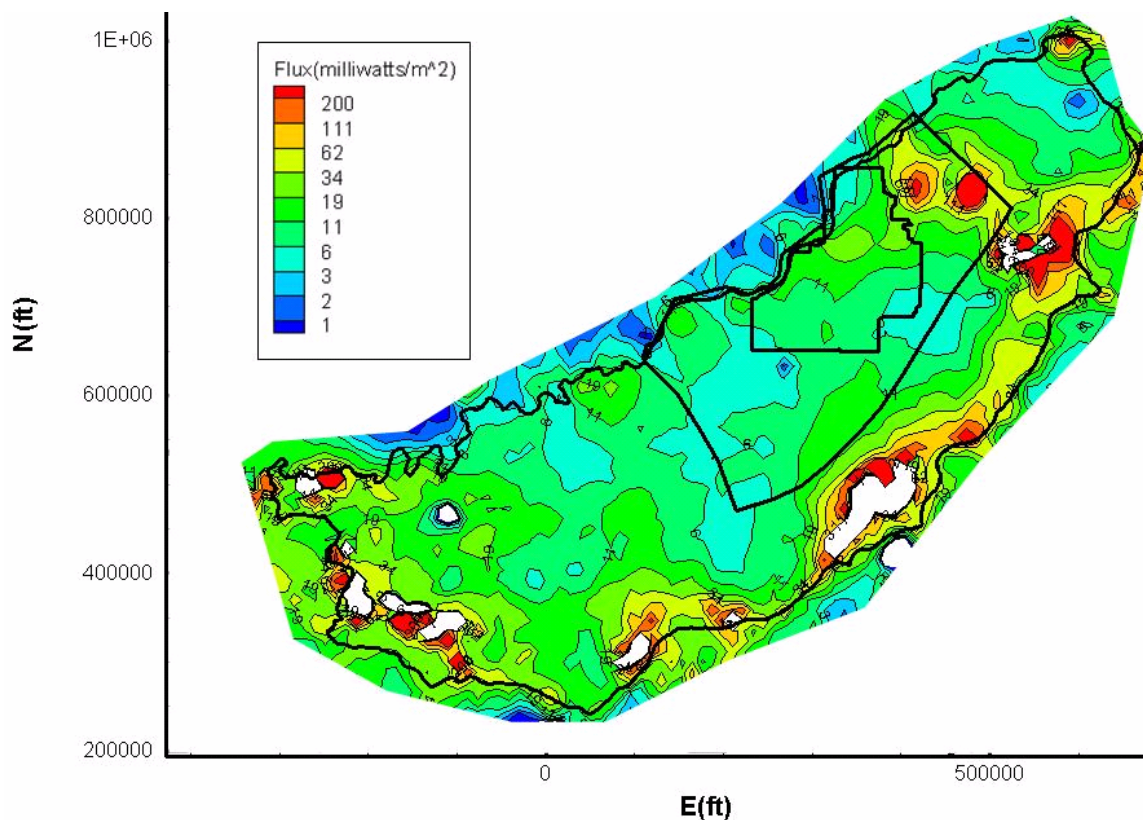


Figure 2-34. Heat flux above the eastern SRPA, based on the groundwater temperature map presented as Figure 2-33 and mean annual air temperatures obtained from the Spatial Climate Analysis Service. Contour scale is exponential because of several anomalously high heat flux values (red areas). Areas shown in white had negative heat fluxes. With one exception, negative fluxes occurred where the estimated groundwater elevation exceeded the surface elevation that was based on the digital elevation model. Heat flux estimates around those areas should, therefore, be considered uncertain, because small errors in elevations at those locations would produce large differences in the calculated heat flux. Solid lines indicate the boundaries of the INL Site, the OU 10-08 study area, and the eastern SRPA.

The heat flux map provides a better indication of the effect of groundwater movement and local recharge on the temperature field than the temperature map itself, because the calculation reflects the effect of the overlying material on the groundwater temperature. Warm anomalies to the northeast of the site, where the unsaturated zone is relatively thin, thus indicate pronounced heat fluxes, while the warm anomaly along the AVH to the south of the site, where the thickness of the unsaturated zone locally exceeds 400 m, produces only minor upward heat flux. The heat flux map also underscores the large difference in heat transfer above and below the aquifer. Below the aquifer, measured heat fluxes are approximately 110 milliwatts m^{-2} (Blackwell et al. 1992). With the exception of several anomalously high values in regions that appear to be affected by local recharge, calculated heat fluxes above the aquifer are less than 35 milliwatts m^{-2} . This underscores the strong influence of the rapidly moving and rapidly replaced groundwater on heat flow through the system. Finally, while this map provides a useful means of examining the spatial distribution of vertical heat flux, the map also provides data necessary for development of a three-dimensional thermo-hydraulic model. The upper boundary of the thermo-hydraulic model will likely be the top of the aquifer. The vertical heat flux map thus provides the upper boundary condition for heat flow in that model.

2.3.3.3 Apparent Sources and Sinks. The groundwater temperature map suggests that temperatures in several locations in the vicinity of the INL Site might greatly aid in constraining groundwater velocities. The most prominent temperature anomalies in the vicinity of identified contaminant plumes are the cold water anomalies located near the spreading areas and beneath Big Southern Butte. The latter might reflect either cold water recharge from the nearby spreading areas or cold water recharge through Big Southern Butte. Using estimates of the likely recharge in the microclimate associated with the butte, as well as information about the spreading areas, we anticipate that we will be able to identify the most likely source. Because we can estimate the recharge flux and the groundwater temperature reasonably well for both sources, heat transport modeling of those effects should provide valuable information about groundwater flow in that area.

Other areas where both recharge fluxes and recharge temperatures should be reasonably well constrained include areas where tributary stream leakage appears to heavily influence groundwater temperature, for example, near the confluence of the North and South forks of the Snake River and along the boundary of the study area where streams flow onto the ESRP.

2.3.3.4 Vertical Temperature Profiles. Temperature data are one of the few existing sources of information about the three-dimensional nature of flow in the eastern SRPA, because temperature logs have been obtained from numerous boreholes that penetrate well below the water table. As part of the OU 10-08 effort to use temperature data to help constrain aquifer velocities, these profiles have been combined with the previously described two-dimensional temperature distribution to develop a three-dimensional picture of temperature distribution below the ESRP. A preliminary fence diagram illustrating the three-dimensional temperature distribution (Figure 2-35) has been generated from about 150 temperature logs, most of which were conducted by Dr. David Blackwell as part of geothermal studies of the area. This fence diagram depicts the approximate extent of the three-dimensional data set available as a target for the three-dimensional heat flow modeling study. Because relatively few wells penetrate to great depth and most of those wells are located on the INL Site, the data density is greatest in that area. INL Site cross sections describing general characteristics of heat flow along and perpendicular to the direction of groundwater flow have previously been described by Smith et al.^c

Temperature profiles have also been used to help identify the bottom of the active portion of the aquifer at the INL Site,^c because vertical temperature gradients within the active flow system are generally much less than those in the subaquifer or in the overlying vadose zone.

The temperature log of the Middle-1823 well illustrates several features common to temperature profiles at the INL Site (Figure 2-36). Immediately above the water table, temperature gradients are relatively steep and appear to reflect diffusive heat transport. Closer to the surface, reversing gradients are frequently observed, probably reflecting seasonal temperature changes that can propagate to a relatively great depth in the fractured basalt stratigraphy. Below the water table, and often extending several hundred yards below, temperature gradients are typically very small. Morse and McCurry (2002) described this as the effect of actively circulating water on the temperature profile. Below this “isothermal” region, the temperature gradient becomes relatively steep and constant to depth. Based on measured values of the thermal conductivity of basalt, this lower regime clearly reflects diffusive heat transport. Based on the measured gradients in such subaquifer sections, the average geothermal heat flux is approximately 110 milliwatts m⁻² (Blackwell et al. 1992).

c. Smith, R. P., T. McLing, and, M. Rohe, 2000, *Implications of Water Temperature, Water Chemistry, and Regional Geophysical Setting for Flow Characteristics of the Snake River Plain Aquifer beneath the INEEL Area*, INL Internal Report.

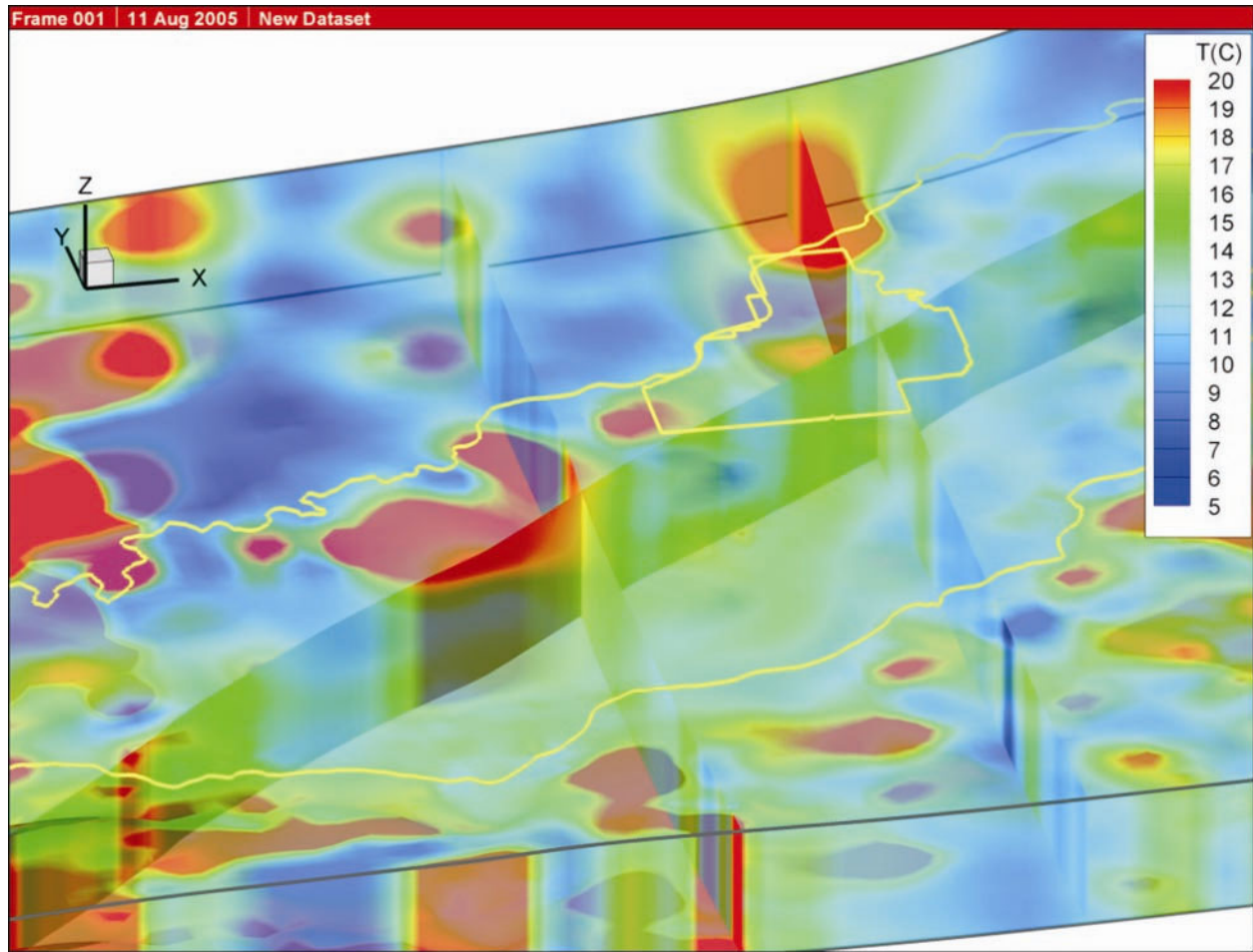


Figure 2-35. Three-dimensional contour plot with vertical cross sections displayed at three arbitrary locations, illustrating the nature and extent of three-dimensional temperature data in the eastern SRPA. The surface of contoured domain is the water table. The thickness of the contoured domain is 610 m (2,000 ft). Interpolated data combine temperature profiles from approximately 150 temperature profiles with the estimated water surface temperature map included as Figure 2-33.

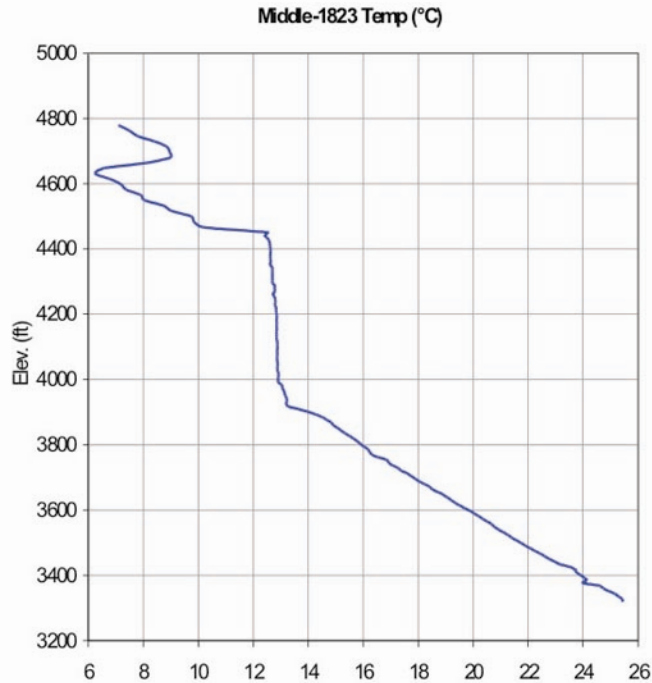


Figure 2-36. Temperature profile obtained in February 2003 from the Middle-1823 corehole.

As part of an effort to further define the large-scale hydrostratigraphy, temperature profiles are currently being reviewed to separate intra-borehole flow effects from the effects of natural groundwater flow on temperatures. Within the isothermal section of several INL Site wells, changes in gradient are commonly observed, and, in some cases, these changes might be indicative of hydrostratigraphic breaks. Intra-borehole flow can produce similar effects in uncased wells. For example, water is free to enter or exit the open borehole in response to variations in vertical head differences across hydrogeologic units and fracture networks (Figure 2-37). In this manner, the natural groundwater flow system can be short-circuited by flow within the borehole. The velocity of water flowing in the open borehole is likely to be fast enough so that diffusive heating is insufficient to bring the moving water into equilibrium with the natural system. Thus, intra-borehole flow can create an isothermal interval in the temperature log that is not representative of the actual temperature profile of the aquifer. Several interpretative techniques are employed to evaluate the effects of intra-borehole flow.

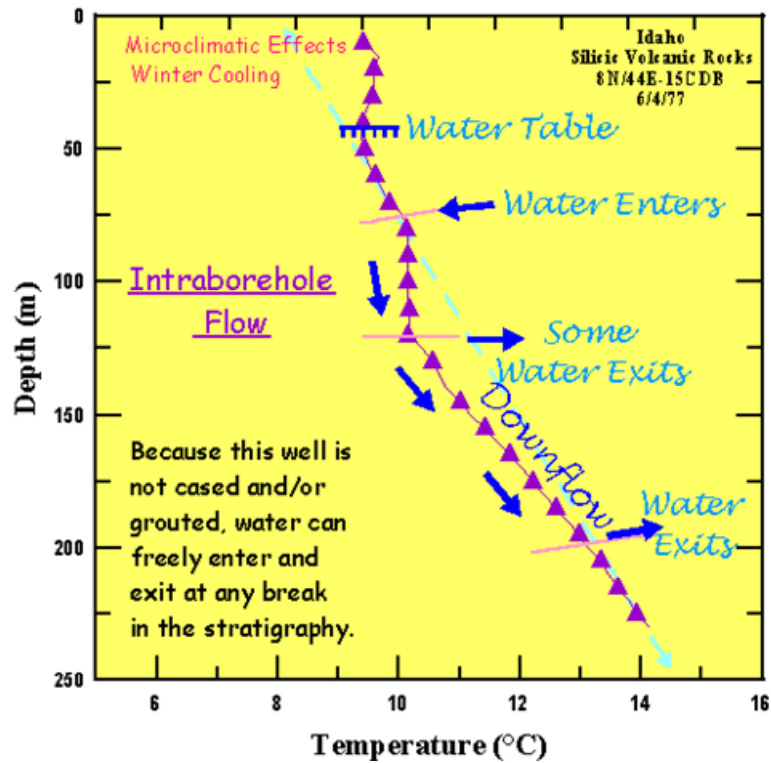


Figure 2-37. Illustration of the effects of intra-borehole flow on the temperature profile of an uncased borehole (from Southern Methodist University [2005]).

